

The influence of vehicle front-end design on pedestrian ground impact

Authors: Gianmarco Crocetta^{1a, b}, Simone Piantini^a, Marco Pierini^a and Ciaran Simms^b

^a *Department of Industrial Engineering, University of Florence, Via di Santa Marta 3, 50139, Firenze, Italy*

^b *Department of Mechanical and Manufacturing Engineering, Parsons Building, Trinity College Dublin, College Green, Dublin 2, Ireland*

Abstract

Accident data have shown that in pedestrian accidents with high-fronted vehicles (SUVs and vans) the risk of pedestrian head injuries from the contact with the ground is higher than with low-fronted vehicles (passenger cars). However, the reasons for this remain poorly understood. This paper addresses this question using multibody modelling to investigate the influence of vehicle front height and shape in pedestrian accidents on the mechanism of impact with the ground and on head ground impact speed. To this end, a set of 648 pedestrian/vehicle crash simulations was carried out using the MADYMO multibody simulation software. Impacts were simulated with six vehicle types at three impact speeds (20, 30, 40 km/h) and three pedestrian types (50th% male, 5th% female, and 6 yr old child) at six different initial stance configurations, stationary and walking at 1.4 m/s.

Six different ground impact mechanisms, distinguished from each other by the manner in which the pedestrian impacted the ground, were identified. These configurations have statistically distinct and considerably different distributions of head-ground impact speeds. Pedestrian initial stance configuration (gait and walking speed) introduced a high variability to the head-ground impact speed. Nonetheless, the head-ground impact speed varied significantly between the different ground impact mechanisms identified and the distribution of impact mechanisms was strongly associated with vehicle type. In general, impact mechanisms for adults resulting in a head-first contact with the ground were more severe with high fronted vehicles compared to low fronted vehicles, though there is a speed dependency to these findings. With high fronted vehicles (SUVs and vans) the pedestrian was mainly pushed forward and for children this resulted in high head ground contact speeds.

Keywords

Vehicle-pedestrian collision, Ground impact; Bonnet leading edge height; Head-ground impact speed; Ground impact mechanism.

¹Corresponding author: Gianmarco Crocetta. Address: Department of Industrial Engineering, University of Florence, Via di Santa Marta 3, 50139, Firenze, Italy.

Email: gianmarco.crocetta@gmail.com

30 The World Bank estimates that each year 1.2 million pedestrians die in road accidents, 35% of which are children (World Bank
31 2002, Lopez *et al.* 2006). The Pedestrian Crash Data Study (PCDS) database in the United States shows that injuries to the lower
32 extremities and head are the most frequent in pedestrian accidents, with head injuries being usually the most severe (Jarrett and
33 Saul 1998, Chidester and Isenberg 2001). An epidemiology study showed that pedestrians struck by an SUV are twice as likely to
34 sustain brain injury as pedestrians struck by passenger cars (Ballesteros *et al.* 2004). The main source of head injuries is the
35 bonnet in SUV accidents but the windscreen dominates in passenger car accidents (Longhitano *et al.* 2005). Comparing dummy
36 and Post Mortem Human Surrogates (PMHS) impact tests with an SUV and a small-sedan at 40 km/h Kerrigan *et al.* (Kerrigan *et*
37 *al.* 2005a, Kerrigan *et al.* 2005b, Kerrigan *et al.* 2012) found that the velocity/HIC score at head strike for a sedan was greater
38 than for an SUV and the increased potential for head injuries shown by accident data (Ballesteros *et al.* 2004) was attributed to
39 the greater stiffness of the bonnet region struck in SUV cases compared to the windscreen struck in car cases. Full scale cadaver
40 tests with a mid-sized sedan and a small city car showed that the whole body kinematics and injury pattern is strongly affected by
41 the kinematics of the pelvis during the vehicle-pedestrian interaction which depends on the pedestrian stature relative to the
42 vehicle front geometry (Subit *et al.* 2008).

43 As seen above, most research efforts have focused on minimising injuries arising from the primary impact with the vehicle.
44 Nonetheless, despite uncertainty in attributing injuries to vehicle or ground contact, accident data show that pedestrian ground
45 contact injuries are also significant. Otte *et al.* (Otte and Pohlemann 2001) analysed 293 pedestrian impact cases and found that
46 injuries could be attributed to ground contact in 66% of cases, and in 11% of cases they were the most severe. They also pointed
47 out that head injuries were more frequent and more severe for vehicle Bonnet Leading Edge (BLE) heights above 700 mm and in
48 the vehicle impact speed range between 20-40 km/h. Similarly, a study of 522 cases from the US Pedestrian Crash Data Study
49 (Roudsari *et al.* 2005) found that in 21% of cases injuries could solely be attributed to ground contact, and that ground impact was
50 the main cause (39%) of head injuries for adults struck by Light Truck Vehicles (LTVs).

51 Pedestrian ground contact mechanisms are highly variable, but in recent years studies have been conducted to investigate the
52 mechanism of injury generation from pedestrian contact with the ground (Kendall *et al.* 2006, Simms and Wood 2006c, Simms
53 and Wood 2006d, Simms *et al.* 2011). These have focused on head injuries, since these are both frequent and the most severe
54 (Jarrett and Saul 1998). Simms and Wood performed multibody simulations of pedestrian impacts with a saloon car and an SUV.
55 They found that, while head injuries from vehicle impact were strongly dependent on impact velocity, injuries from ground
56 impact were variable but mainly influenced by pedestrian head drop height and not by vehicle speed (Simms and Wood 2006a).

57 Similarly, Kendall *et al.* performed impact simulations of the MADYMO multibody pedestrian model with FE models of a
58 small sedan car and an SUV. Overall the vehicle appeared to be more likely to cause injuries than the ground, but the ground was
59 still the main cause of injuries in 25% of cases. In addition, the severity of ground related injuries with respect to vehicle-related

60 injuries was found to be higher with the SUV than with the car (Kendall *et al.* 2006). Simms et al simulated impacts with
61 pedestrian models of a mid-size male and a small female with six vehicle types at speeds between 25 and 35km/h. They found
62 that vehicles with high bonnet leading edges such as SUVs were more likely to lead to a direct head impact with the ground
63 compared to lower fronted vehicles (Simms *et al.* 2011). In addition six recurring pedestrian-ground impact mechanisms were
64 observed in 94% of the 72 simulated cases. However, in this preliminary study the vehicle shapes were approximate, the speed
65 range was limited and although the influence of gait on pedestrian kinematics is well established (Elliott *et al.* 2012), only two
66 gait stances were considered.

67 Gupta et al. simulated impacts of a mid-size male, a small female and a 6 yr old child against FE models of a sedan car and an
68 SUV (Gupta and Yang 2013) and found that a lowered car front profile and a raised SUV front profile prevented direct head
69 impact with the ground. In contrast, a raised-front car profile and a lowered-front SUV profile led mainly to head-first impacts
70 with the ground, but it was unclear why this occurred.

71 In the aforementioned studies (Kendall *et al.* 2006, Simms and Wood 2006a, Simms *et al.* 2011, Gupta and Yang 2013) the
72 head injury risk evaluation was performed by calculating the HIC scores from impacts with the vehicle and the ground. However,
73 the Madymo multibody pedestrian model is not yet validated for the prediction of head injuries from the impact with the ground,
74 and results are very sensitive to the contact stiffness in the modelling. A kinematic approach followed by Hamacher et al.
75 (Hamacher *et al.* 2012) in a multibody computational investigation found that SUVs and vans were associated with higher
76 projection distances, and the authors concluded that high-fronted vehicles therefore pose a higher risk of pedestrian head injuries
77 from the ground contact.

78 Overall, a biomechanical analysis of the relationship between pedestrian head ground injuries and vehicle type remains
79 incomplete. The objective of the present paper is therefore to use a multibody computational approach to evaluate whether the
80 ground impact mechanisms identified by (Simms *et al.* 2011) could be clearly identified even when a more representative set of
81 vehicle shapes, and a broader range of vehicle impact speeds and pedestrian initial positions is considered. Moreover, this work
82 aimed at assessing whether a relation could be identified between the pedestrian ground impact configuration (head first, pelvis
83 first etc.) and vehicle front shape and height as assessed by Bonnet Leading Edge height.

84 **2 - Methods**




85 *2.1 - Pedestrian models*

86 The 50th % male, 5th % female and the 6 yr-old child MADYMO multibody pedestrian models (MADYMO 2011) were applied in
87 a vehicle pedestrian impact with the initial pedestrian orientation perpendicular to the direction of vehicle travel (i.e. the
88 pedestrian was struck from the left). The main features of the used pedestrian models are shown in Table 1. These three
89 pedestrian models were chosen to have a wider representation of road users. Since the simulations were analysed individually, the

90 number of employed pedestrian models was limited to three in order to attain a reasonable analysis time. The 50th % mid-size
 91 male pedestrian model was preferred to the 95th % male pedestrian as it has been extensively validated in (Van Rooij *et al.* 2003,
 92 Anderson *et al.* 2007) for the reproduction of pedestrian impacts and the analysis of vehicle contact. The model has recently been
 93 compared to staged tests and a real collision in terms of head trajectory, longitudinal and transverse head translation relative to the
 94 primary contact location of the pedestrian on the vehicle, impact location on the head, head impact time and head impact velocity
 95 (Elliott 2011). The results showed that the model can be used to quantitatively test the influences of pre-impact vehicle speed,
 96 pedestrian speed and pedestrian stance on pedestrian kinematics during the interaction with the vehicle (Elliott *et al.* 2012).
 97 Attempts have also been made to validate the pedestrian models in MADYMO by reconstructing real collisions. Linder et al.
 98 (Linder *et al.* 2005) used the MADYMO pedestrian model to simulate real accidents and compared the response of simulations to
 99 collision data in terms of head impact location and pedestrian throw distances (within 20% of the estimated values from post-
 100 collision data). Yao et al. (Yao *et al.* 2008) used the pedestrian model in MADYMO to reconstruct 10 real-world collisions
 101 finding a good correspondence with the collision data in terms of pedestrian wrap-around distance (errors of 2–4%) and
 102 pedestrian throw distance (errors of 0–16%).

103 The 5th % female and the 6 yr-old child models were obtained by scaling the 50th % male model using MADYMO/SCALER
 104 (Happee *et al.* 1998). No direct validation data of the 5th % female and the 6 yr-old child models are available yet.

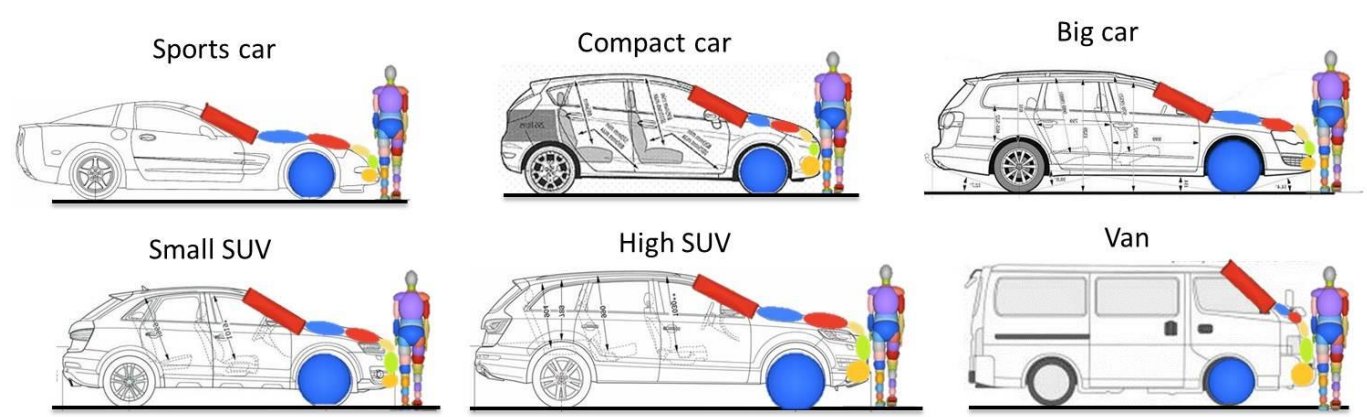
106 **Table 1. MADYMO pedestrian models**

	6-year old child	5th percentile female	50th percentile male
			
Height [m]	1.17	1.53	1.74
CG height [m]	0.665	0.843	0.958
Weight [kg]	23.0	49.8	75.7

108 **2.2 - Vehicle models**

109 The front shapes of six vehicle types were modelled in MADYMO with 5 extruded cylinders and one ellipsoid. The models,
 110 shown in Fig. 1, were based on actual vehicles representative of six categories: a sports car, a compact car, a big car, a small
 111 SUV, a big SUV and a van. The vehicles were characterized by bonnet leading edge (BLE) increasing in height from the sports
 112 car to the van but also having different bonnet angles and length, see Table 2. The bonnet leading edge is defined according to the
 113 EuroNCAP protocol as the front upper outer structure of the vehicle including the bonnet and wings, the upper side members of

114 the headlight surround and any other attachments (EuroNCAP 2013). In Table 3 are shown for each vehicle the values of the ratio
 115 “bonnet leading edge height/pedestrian centre of gravity height” and of the ratio “bonnet leading edge height/pedestrian height”.
 116



117 **Fig. 1. MADYMO models of the vehicles and 50th % male pedestrian model.**

118 **Table 2. Geometrical dimensions of vehicle fronts.**

119

120

Vehicle	Sports car	Compact car	Big car	Small SUV	Big SUV	Van
Bonnet length (mm)	1454	795	1080	1026	1272	330
Bonnet angle (°)	4	13	7	11	8	31
BLE height (mm)	535	694	725	795	942	1050
Ground clearance (mm)	185	230	258	297	304	280
Windscreen angle (°)	28	28	27	31	27	43

121

122 **Table 3. Ratio vehicle bonnet leading edge height/pedestrian centre of gravity height and vehicle bonnet leading edge**
 123 **height/pedestrian height**

124

Vehicle BLEH/Ped.C.G. Height	Sports car	Compact car	Big car	Small SUV	Big SUV	Van
6-year old child	0.805	1.044	1.090	1.195	1.417	1.579
5th percentile female	0.635	0.823	0.860	0.943	1.117	1.246
50th percentile male	0.558	0.724	0.757	0.830	0.983	1.096
Vehicle BLEH/Ped Height						
6-year old child	0.457	0.593	0.619	0.679	0.805	0.897
5th percentile female	0.349	0.453	0.473	0.519	0.615	0.686
50th percentile male	0.307	0.398	0.416	0.456	0.541	0.603

125 **2.3 - Contact characteristics**

126 MADYMO is a commercial multibody simulation software package in which systems of rigid bodies connected by kinematic
 127 joints are allowed to contact and penetrate each other. Contact forces are computed according to specified contact characteristics.

128 The loading and unloading curves for the present study were sourced from a study by Lyons and Simms (Lyons and Simms
129 2012). The loading functions for the bumper and the bonnet provided by Lyons and Simms were based on a paper from Liu et al.
130 (Liu *et al.* 2002), while the windscreen stiffness was extracted from the impactor tests of Mizuno and Kajzer (Mizuno and Kajzer
131 1999). The unloading curves for bumper, bonnet and windscreen were based on 10% of the stiffness of the corresponding loading
132 curves and the unloading curve for the BLE was based on 1% of the stiffness of the BLE loading curve.

133 A friction coefficient of 0.3 for the vehicle-pedestrian contacts was used as previous studies found that it gave reasonable results
134 (Simms and Wood 2006a, d). The hysteresis slope was set to 10^8 for all vehicle contacts. The combined force-deformation
135 characteristics of both contacting surfaces were used in all contacts except for the vehicle-head contact, in which only the vehicle
136 deformation characteristics were used.

137 As regards the pedestrian-ground interaction, no validated contact model is available yet. Therefore, only the pedestrian contact
138 characteristics were used and the ground was modelled as a rigid surface. To model the friction force in the contact with a dry-
139 asphalt road a friction coefficient of 0.58 for the pedestrian-ground interaction was chosen, based on experimental test results
140 (Wood and Simms 2000).

141 2.4 - *Impact conditions*

142 Impact simulations were performed for three initial vehicle velocities: 20, 30 and 40 km/h to reproduce the range of typical
143 impact speeds in pedestrian accidents (Simms and Wood 2006c). Very high speeds were not considered since survivability
144 following primary contact with the vehicle is then low. A constant deceleration of 0.75g was applied to the vehicles to simulate
145 braking at impact on a dry-asphalt surface, similarly to the approach taken in previous studies (Simms and Wood 2006b, Simms
146 *et al.* 2011). Vehicle dipping during the braking due to suspensions compression and tyres deformation was neglected as done in
147 previous studies (Van Rooij *et al.* 2003, Simms and Wood 2006a, Shen *et al.* 2008, Untaroiu *et al.* 2010, Elliott *et al.* 2012).

148 Six initial stance configurations were chosen from the gait cycle defined by Untaroiu et al. (Untaroiu *et al.* 2009) with the
149 pedestrian facing sideways to the vehicle. The selected stance configurations are those circled in Fig. 2: the struck leg was leading
150 in three cases (0%, 10%, 80%) and lagging in the other three (30%, 50%, 60%). Impacts were performed with the pedestrian both
151 stationary and moving transversally to the vehicle at a (walking) speed of 1.4m/s (Simms and Wood 2006c), though the full
152 complexities of walking were not modelled. The simulation parameters are summarized in Table 4. A total of 648 multibody
153 simulations of vehicle-pedestrian impacts was carried out using MADYMO.

154 There are currently no experimental data for validation of pedestrian ground contact kinematics and injuries. Accordingly, the
155 predictive capabilities of the MADYMO pedestrian model for ground contact assessment cannot currently be tested. To address
156 this limitation, the results presented from this work focus on trends rather than absolute values of head impact speed predictions.
157

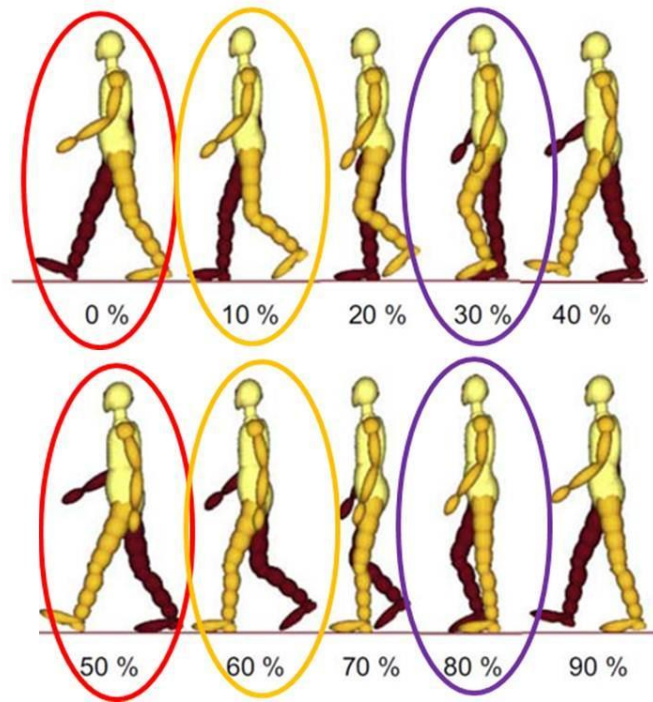


Fig. 2. Initial pedestrian stances simulated. Adapted from (Untaroiu et al. 2009).

Table 4. Simulation matrix

	Vehicle type	Vehicle impact speed (m/s)	Pedestrian model	Pedestrian gait position	Pedestrian initial speed (m/s)
	sports car, compact car, big car, small SUV, big SUV, van	5.5, 8.3, 11.1	50 th % male, 5 th % female, 6 y.o. child	0%, 10%, 30%, 50%, 60%, 80%	0, 1.4
Total	6	3	3	6	2

2.5 - Analysis Approach

Impact kinematics were studied to identify patterns of body stance and motion at the instant of ground contact. The analysis of how vehicle shape influences the ground impact severity was carried out by identifying the head-ground impact speed as the absolute value of the vertical component of the head's centre of gravity velocity at impact with the ground. For each impact mechanism the average head-ground impact speed was used to assess the relative severity of the different configurations of impact. The possible existence of identifiable relationships of head-ground impact speed and time to head-ground contact with the bonnet leading edge height was also investigated.


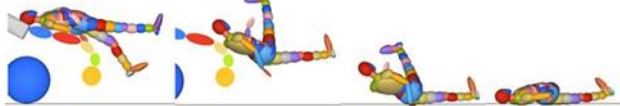


171 **3 - Results**

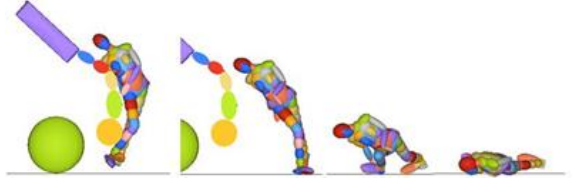
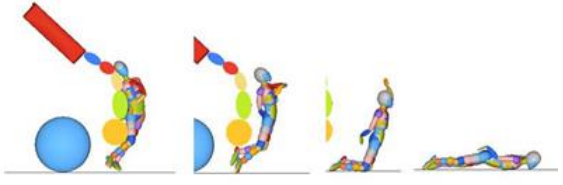
172 The graphic animations of each simulation were analysed to classify the pedestrian post-impact kinematic and the type of ground
 173 impact configuration. The head-ground impact speed for each case was calculated at the simulation time step preceding the one in
 174 which head-ground contact force became different from zero.

175 *3.1 - Identification of impact mechanisms*

176 Out of a total of 648 simulations, in 617 cases (95%) it was possible to identify six recurring ground impact mechanisms,
 177 distinguished from each other by the type of pedestrian post-impact trajectory (wrap or forward projection), direction of body
 178 rotation prior to ground impact and manner in which the pedestrian impacted the ground, see Table 5 and Fig. 3. The remaining
 179 31 cases (5%) could not be clearly classified in any of the six categories or were excluded because pedestrian limbs shielded the
 180 head impact with ground altering the head-ground impact kinematics.

181
 182
 183 **Table 5: Description of the identified impact mechanisms.**

<p>Mechanism 1</p>	<p>This is a wrap trajectory, in which the head hits the ground first. The pedestrian rotates between 90° and 180° before ground impacting the ground in a head-first configuration.</p>	
<p>Mechanism 2</p>	<p>The kinematics are similar to Mechanism 1 but there is less rotation of the body and the pelvis strikes the ground first, followed by the legs and head. The angle of rotation of the pedestrian is less than 90°.</p>	
<p>Mechanism 3</p>	<p>As in Mechanism 1, the head strikes the ground first, but the pedestrian rotates through more than 180° before impacting the ground.</p>	
<p>Mechanism 4</p>	<p>In Mechanism 4 the body rotates more than 270° before impacting the ground. The pelvis or legs strikes the ground first, followed by the</p>	

	torso and the head.	
Mechanisms 5a	Mechanism 5a is a forward projection in which the pedestrian is pushed in the direction of vehicle travel with the legs contacting the ground first. In this case (3% of cases) the head contacts the ground with whole body rotation towards the vehicle front.	
Mechanism 5b	Mechanism 5b is a forward projection too. In this case (11% of cases) the head contacts the ground with whole body rotation away from the vehicle front.	

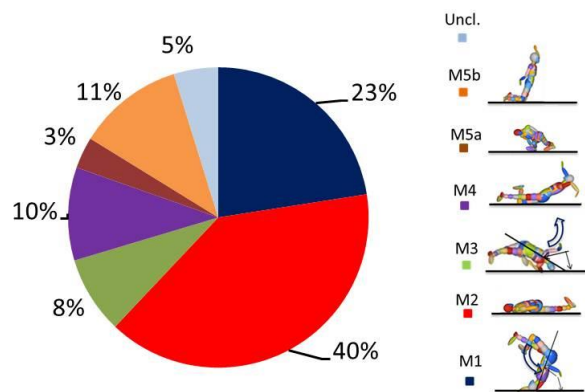


Fig. 3. Breakdown of impact mechanisms.

3.2 - Relationship between impact mechanism and head ground impact speed

The average and standard deviation of the head-ground impact speed distributions for each Mechanism is shown in Table 6, Fig. 4 and separately for the three vehicle impact speeds in Fig. 5. An ANOVA single factor performed on the six classes represented by the ground impact Mechanisms gave an F ratio of 100.7 with an F critical of 2.1 and a P-value < 0.001. This result indicates that the values of head-ground impact speed within each of the six Impact Mechanism categories are statistically distinct and considerably different. (Moore and McCabe 2003).

Table 6. Average head-ground impact speed for impact mechanism.

Impact Mechanism	Avg. head-ground speed (m/s)	Standard deviation (m/s)
1	4.73	0.75
2	3.23	1.39
3	2.93	0.59
4	5.21	1.71
5a/5b	1.96	0.95
5b	6.05	1.01

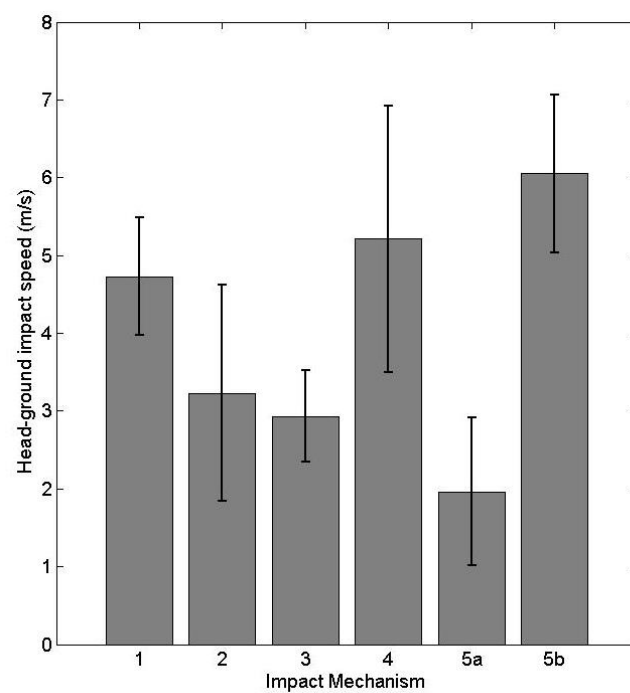


Fig. 4. Average values and standard deviations of head-ground impact speed for each impact Mechanism for all pedestrian models.

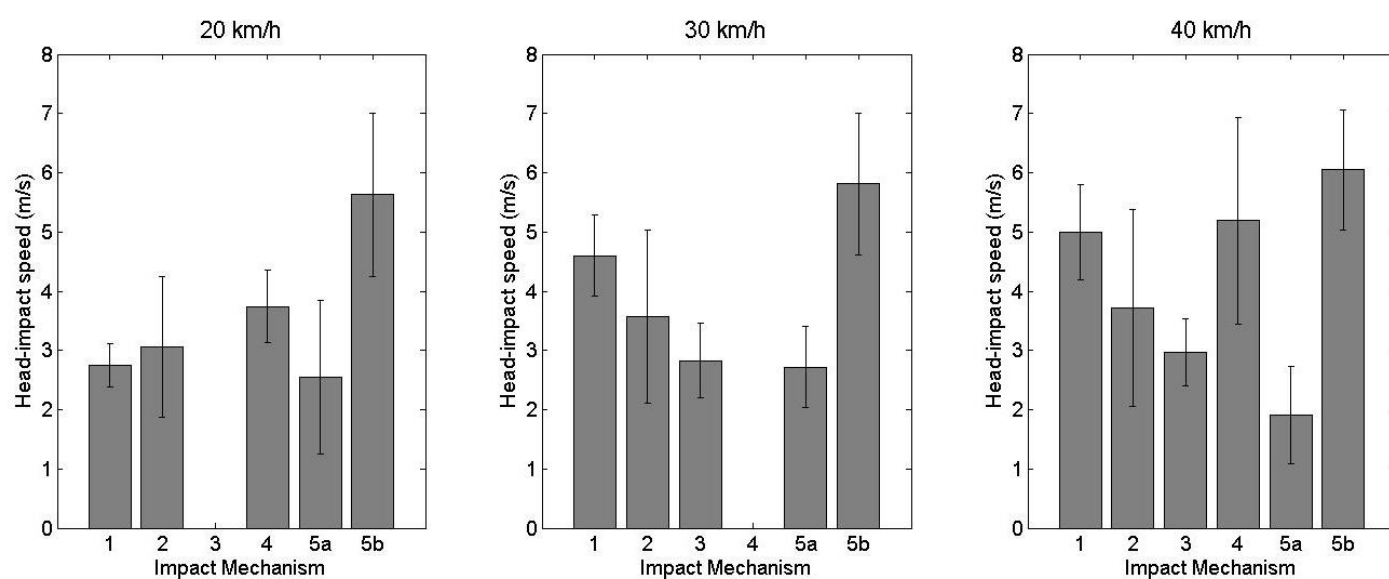


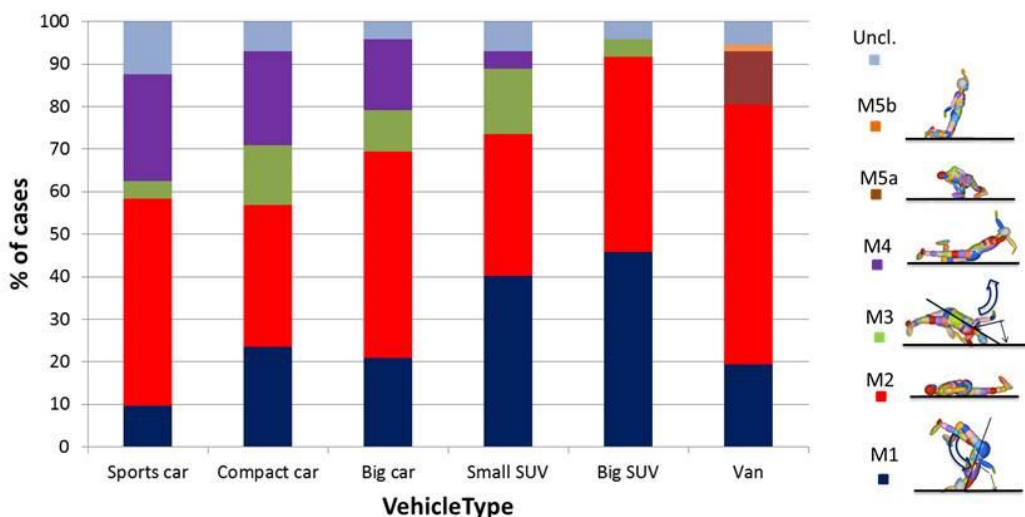
Fig. 5. Average values and standard deviations of head-ground impact speed for each impact Mechanism at the three vehicle impact speeds for all pedestrian models.

205 3.3 - Relationship between impact mechanism and vehicle type

206 Due to the large difference in stature between the two adult pedestrian models (mid-size male and small female) and the child
207 pedestrian model the post impact kinematics experienced by adult and child pedestrians differed significantly. Accordingly, the
208 distributions of impact mechanisms for the different vehicle types are presented separately for the two adult pedestrians and for
209 the child pedestrian cases.

210 Fig. 6 shows the frequency of the different ground impact mechanisms for adult pedestrians (male and female) at all vehicle
211 impact speeds considered (20, 30 and 40 km/h) while Figs 7-9 show the mechanism frequencies at 20 km/h, 30 km/h and 40 km/h
212 respectively. Similarly, Fig. 10 shows the instances of the different ground impact mechanisms for child pedestrians at all vehicle
213 impact speeds considered (20, 30 and 40 km/h), while Figs 11-13 show the mechanism frequencies for child pedestrians at 20
214 km/h, 30 km/h and 40 km/h respectively.

215



216

217 **Fig. 6. Occurrences of the six impact mechanisms for each vehicle type for the adult pedestrian impacts at all vehicle**

218 **impact speeds (20, 30 and 40 km/h).**

219

220

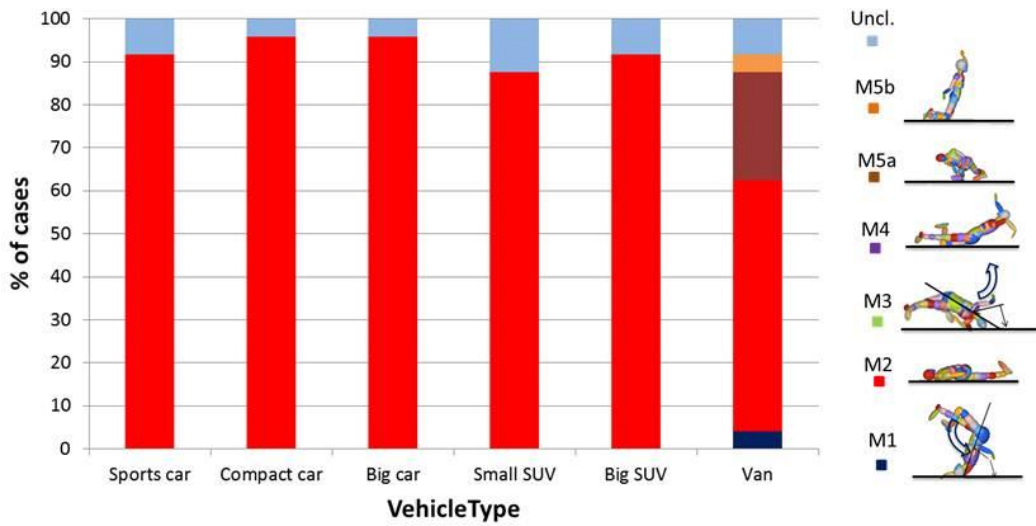


Fig. 7. Occurrences of the six impact mechanisms for each vehicle type for the adult pedestrian impacts at 20 km/h.

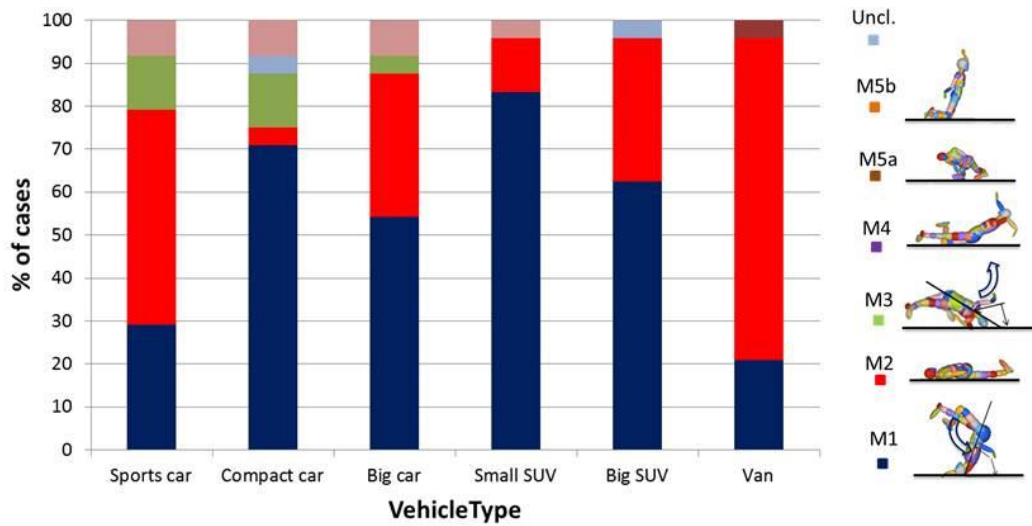
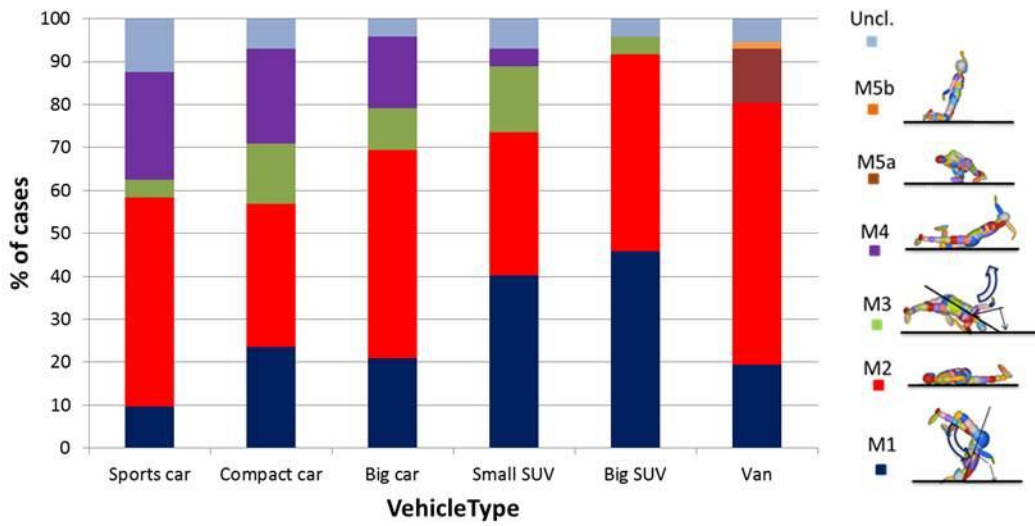
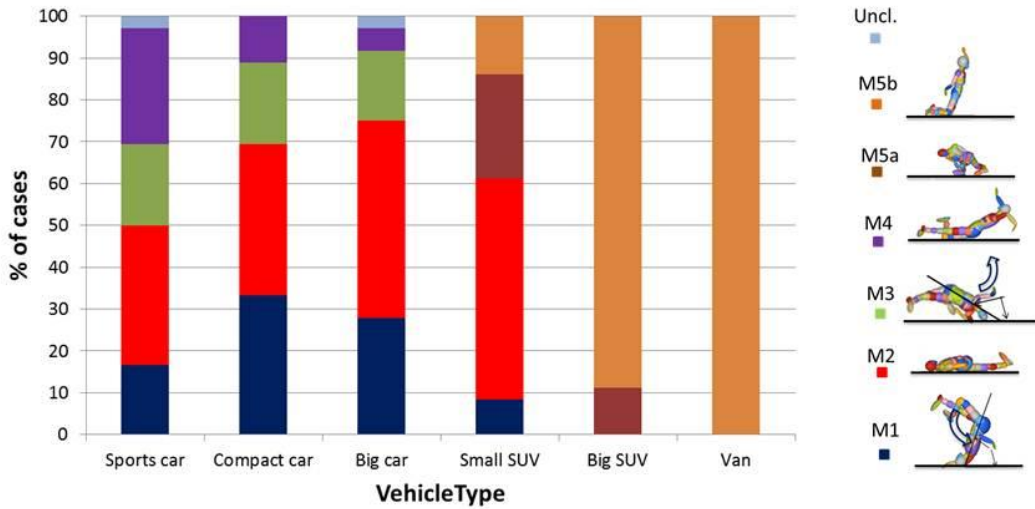


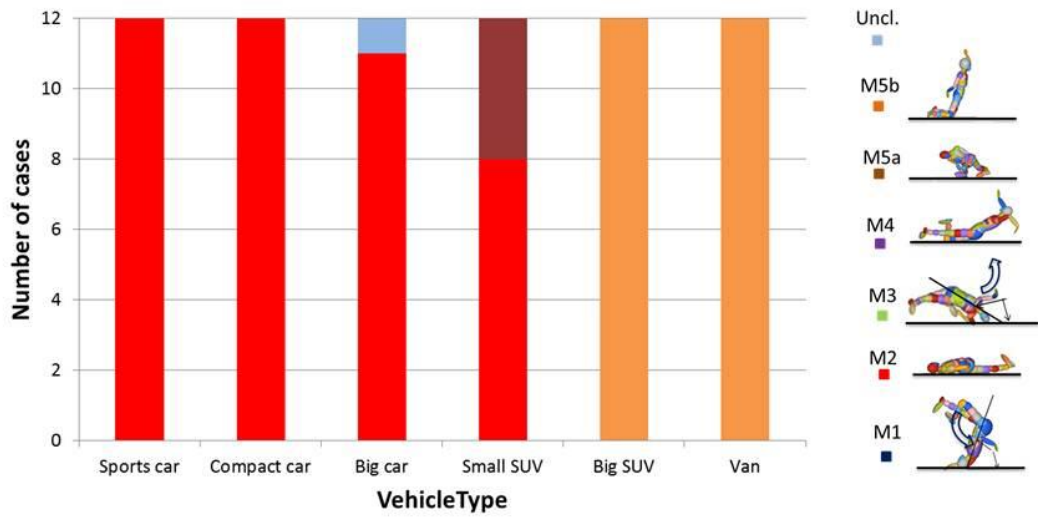
Fig. 8. Occurrences of the six impact mechanisms for each vehicle type for the adult pedestrian impacts at 30 km/h.



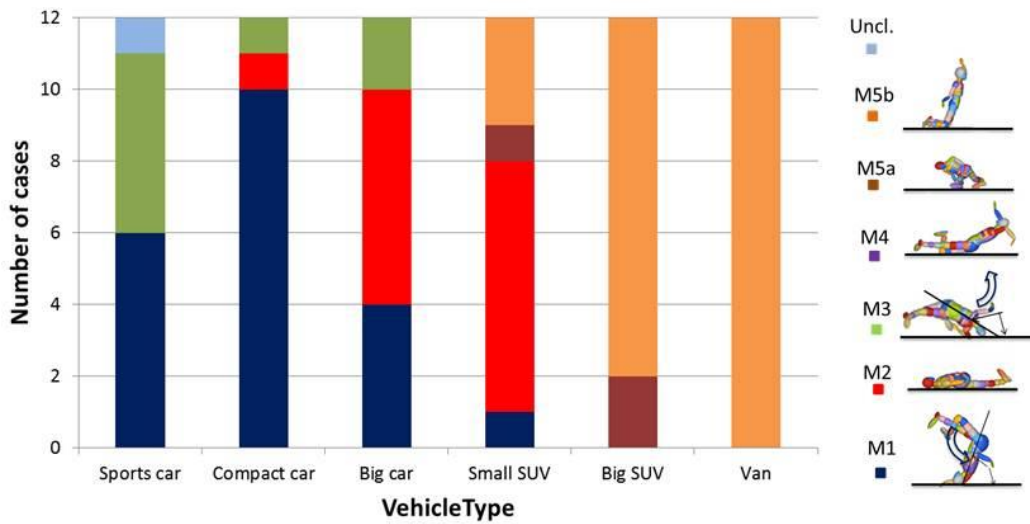
227
228 **Fig. 9. Occurrences of the six impact mechanisms for each vehicle type for the adult pedestrian impacts at 40 km/h.**
229



230
231 **Fig. 10. Occurrences of the six impact mechanisms for each vehicle type for the child pedestrian impacts at all vehicle**
232 **impact speeds (20, 30 and 40 km/h).**
233
234

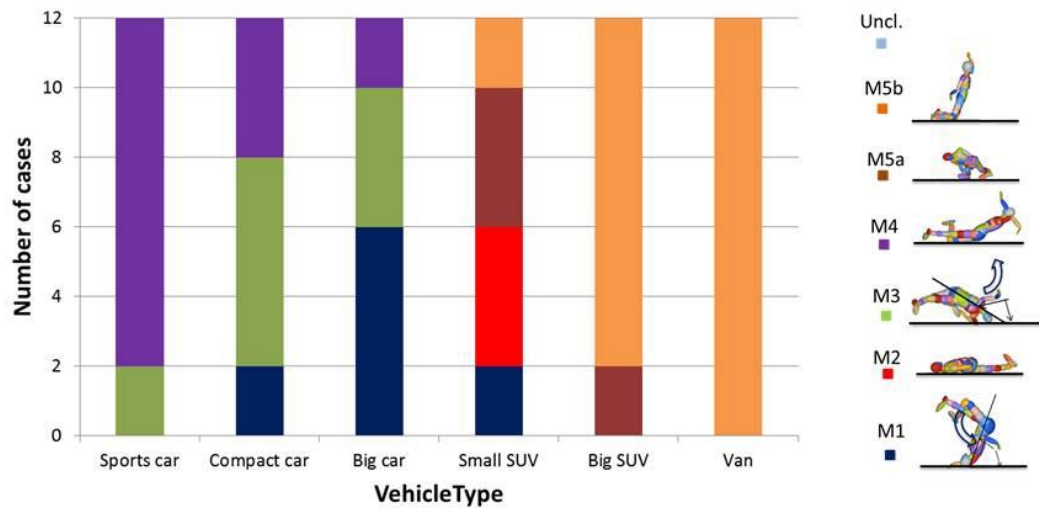


235
236 **Fig. 11.** Occurrences of the six impact mechanisms for each vehicle type for the child pedestrian impacts at 20 km/h.



239
240 **Fig. 12.** Occurrences of the six impact mechanisms for each vehicle type for the child pedestrian impacts at 30 km/h.

241

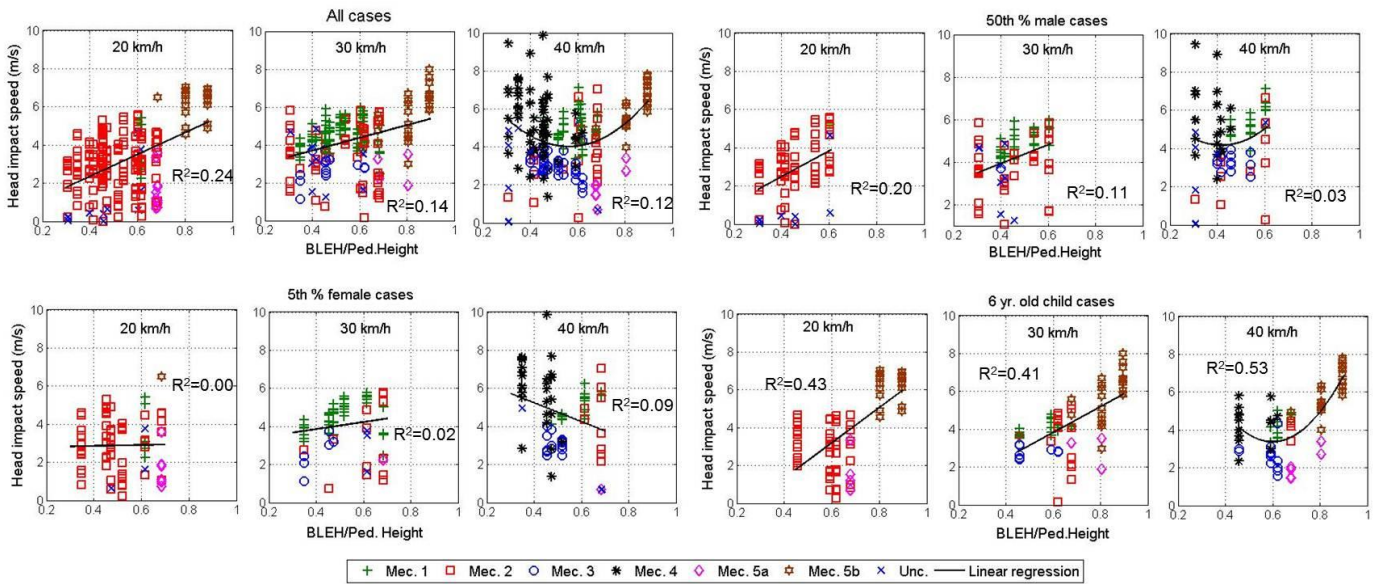


242
243 **Fig. 13. Occurrences of the six impact mechanisms for each vehicle type for the child pedestrian impacts at 40 km/h.**

244 *3.4 - Relationship between head-ground impact speed and normalized bonnet leading edge height*

245 Fig. 14 shows the head-ground impact speed for different vehicle speeds and pedestrian sizes as a function of the vehicle's
 246 normalized bonnet leading edge height (NBLEH), which is the ratio of the Bonnet Leading Edge Height to the pedestrian height.
 247 The data in Fig. 14 are stacked in columns corresponding to specific NBLEH values, with each column obtained from a specific
 248 combination of vehicle type and pedestrian model. Each column contains 12 values of head-ground impact velocity
 249 corresponding to six initial stances and two initial pedestrian speeds (0 and 1.4 m/s). Different markers within each column
 250 indicate the ground impact mechanism. Data located on the horizontal axis are cases where no head-ground impact occurred. R²
 251 for a linear or quadratic regression is given in each case.

252

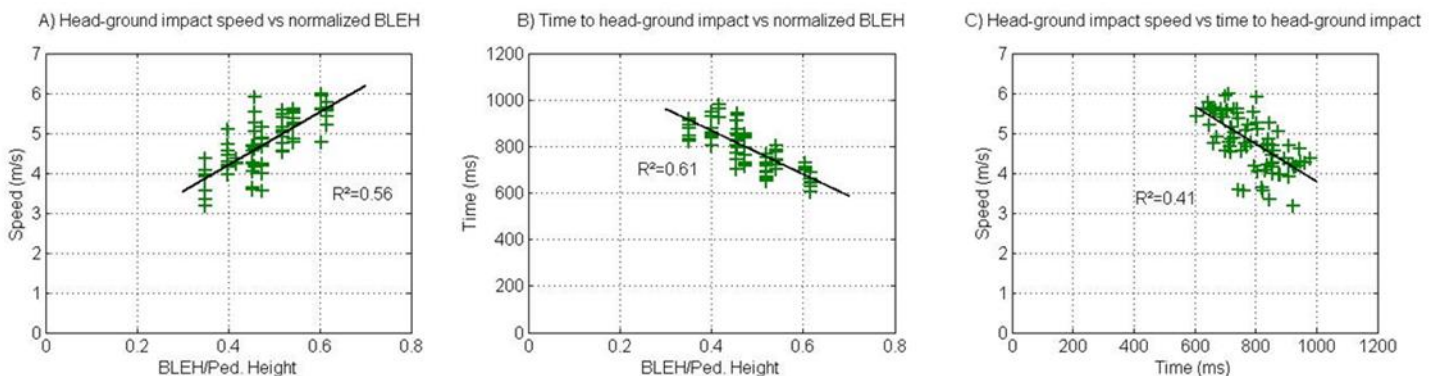


253
 254 **Fig. 14. Head-ground impact speed against normalized bonnet leading edge height (NBLEH) plotted separately for the**
 255 **three vehicle impact speeds. The points stacked on the same column correspond to impact simulations with the**
 256 **same combination of vehicle type and pedestrian type but with different pedestrian initial stance and walking**
 257 **speed. Each marker indicates the identified ground impact mechanism.**

259 For the adult pedestrian cases the highest average head-ground impact speed occurs for Mechanism 4 (5.1 m/s) and Mechanism 1
 260 (4.6 m/s). Mechanism 4 occurs only at 40 km/h while Mechanism 1 occurs mainly at 30 km/h (77 cases, 67%). For these 77 cases,
 261 the head-ground impact speed as a function of NBLEH is shown in Fig. 15 A.

262 For Mechanism 1 cases at 30 km/h the time between first contact with the vehicle and the head-impact with the ground is also
 263 negatively correlated with the NBLEH, see Fig. 15 B, and linear regression again shows high correlation ($R^2 = 0.61$).

264 A similar relationship (Fig. 15 C) exists between the time to head-ground impact and the head-ground impact speed ($R^2 = 0.41$).



266
 267 **Fig. 15. Cases of Mechanism 1 for adult pedestrian impacts at 30 km/h. A) Head-ground impact speed against**
 268 **normalized bonnet leading edge height. B) Time to head-ground impact against normalized BLEH. C) Head-**
 269 **ground impact speed vs time to head-ground impact.**

4 - Discussion

This paper describes the existence of patterns for the influence of pedestrian and vehicle size and speed and pedestrian initial stance on pedestrian head ground contact mechanisms as a precursor to studying pedestrian ground related injury outcome. The analysis is based on 648 MADYMO multibody simulations and the categorisation of the geometric configuration of the pedestrian's body at the instant of head contact with the ground, see Table 5. These categories are largely based on the degree of pedestrian whole-body rotation at the instant of ground contact, as well as whether or not the head is the first body region to contact the ground. Six of these impact mechanisms correspond to those identified in the preliminary study by Simms *et al.* (Simms *et al.* 2011), although Mechanism 5a corresponds to Mechanism 5 of the Simms *et al.* study. The post-impact kinematics described by Mechanism 5b was not observed in the preliminary study (Simms *et al.* 2011) as child pedestrians were not considered.

Table 6 and Fig. 4 shows that Mechanism 1, 4 and 5b have significantly higher head ground contact speeds (4.6 m/s, 5.1 m/s & 6.5 m/s respectively) than Mechanism 2, 3 and 5a (3.2 m/s, 2.9 m/s & 1.9 m/s respectively). Given this significant variation, the following discussion first seeks to provide a kinematic explanation and then to assesses the combined effects of vehicle speed and type, and pedestrian size, gait and speed on the frequency of occurrence of the different ground contact Mechanisms. As already pointed out, the absence of validation data for pedestrian ground contact is a limitation of this work, which means that the focus should be on trends rather than absolute values.

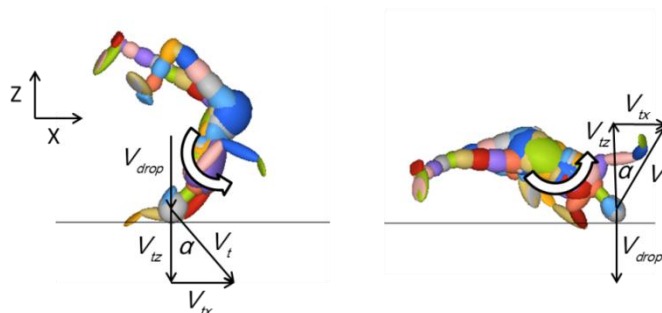
4.1 - *The influence of ground impact mechanism on head ground contact speed*

The high F-ratio (100.7) and the very low P-value ($<1e-10$) associated with the analysis of variance of the data in Fig. 4 indicates that the head-impact speed distribution for each mechanism can be considered statistically different to all other mechanisms. Mechanism 1, 4 and 5 show the highest head impact speeds with the ground (Table 6). In general, the highest head ground impact speed occurs for cases where the whole-body rotation increases the head linear velocity and for cases where there is no shielding of the head contact with the ground through prior contact with other body regions, see Table 5 and Table 6. Thus the average head-ground impact speed for Mechanism 1 (4.6m/s) is higher than for Mechanism 2 (3.2m/s) and Mechanism 3 (2.9m/s). Mechanism 2 mostly occurs at lower impact speeds (66% of cases at 20 km/h, 25% at 30 km/h and 9% at 40 km/h) and therefore the angular velocity induced from vehicle impact is lower than Mechanisms 1, 3 and 4 that occur at higher vehicle impact speeds. This is clearly visible in Table 5 if the typical pedestrian kinematics of Mechanism 1 and 2 are compared. In Mechanism 2 the pedestrian upper body remains almost horizontal for the entire duration of the flight phase, while in Mechanism 1 much more body rotation takes place, indicating a higher angular velocity.

299 For Mechanism 1 and 3, the large difference in average head-ground impact speed is due to the direction of body rotation prior
 300 to head-ground impact. The vertical component of the head velocity can be deconstructed into two contributing parts, as shown in
 301 Fig. 16. The first is the drop velocity (V_{drop}) associated with the downward motion of the whole body due to gravity, and this is
 302 largely determined by the height reached by the body after vehicle impact. The second contribution is the vertical component (V_{tz})
 303 of the head's tangential velocity (V_t) due to whole-body rotation. This depends on α , the angle between the ground and torso at the
 304 moment of head-ground impact. The impact velocity of the head with the ground is therefore given by:

$$306 \quad V_{imp} = V_{drop} + V_{tz} = V_{drop} + V_t \cos \alpha \quad (1)$$

307
 308 Fig. 16 shows that in Mechanism 1 V_{tz} increases the head-ground impact speed. In contrast, for Mechanism 3 whole body rotation
 309 moves the head away from the ground, decreasing the head-ground impact speed. This results in lower average head-ground
 310 impact speeds for Mechanism 3 (2.9 m/s) than for Mechanism 2 (3.2 m/s). Since impact energy is proportional to the square of
 311 speed, this 10% speed difference can be significant.



313
 314 **Fig. 16. Components of head's velocity in Mechanism 1 and 3**

315
 316 The highest head-ground impact speeds were found for Mechanism 5b (6.5 m/s) and Mechanism 4 (5.1 m/s). Interestingly, these
 317 are both ground impact configurations in which the head ground impact is preceded by the impact of pedestrian's lower limbs or
 318 pelvis. For Mechanism 4, the high head-ground impact speed may result from increased whole-body rotation following pelvis
 319 contact with the ground.

320 In Mechanism 5b, the pedestrian is projected forward after the impact with the vehicle, after which the feet or knees strike the
 321 ground and act as pivots for rotation of the body towards the ground, causing part of the horizontal component of pedestrian's
 322 linear momentum to be transferred into rotation towards the ground. This occurred almost exclusively for the child pedestrian
 323 cases when struck by the SUV or van models and leads to the most severe head-ground impact speed (6.5 m/s on average)

amongst all the observed impact mechanisms. Mechanism 5a differs significantly from Mechanism 5b since whole-body rotation is in the opposite direction and head impact with ground occurs at much lower speeds (1.9 m/s on average).

4.2 - *The relationship between normalised bonnet leading-edge height and head ground impact speed*

Fig 14 shows a large variability for head impact speed for each NBLEH ordinate, with values ranging from 0 m/s (no head impact with ground) to almost 10 m/s for the range of pedestrian speeds and gait stances considered. This variability results from the effects of pedestrian initial stance and speed, again highlighting the well-known sensitivity of pedestrian ground contact kinematics to the initial impact conditions (Simms and Wood 2006a, Simms *et al.* 2011).

Fig 14 shows a minor trend towards an increase in head ground impact speed with increasing vehicle speed: the overall average head impact speed increases from 3.2 m/s at 20 km/h to 4.2 m/s at 30 km/h and 4.5 m/s at 40 km/h.

At 20 and 30 km/h, considering all pedestrian sizes, speeds and gait stances, Fig. 14 A shows a weak trend towards increasing head impact speed as a function of normalized bonnet leading edge height (NBLEH). However, the R^2 values for a linear regression analysis are low: 0.24 at 20 km/h and 0.14 at 30 km/h. Furthermore, at 40 km/h a different (also weak) trend is observable: instead of a consistent increase in head impact speed as a function of NBLEH, there is an apparent parabolic relationship, with lowest and highest NBLEHs leading to higher head impact speeds than intermediate ones. However, a quadratic regression yields only $R^2 = 0.12$. This trend results from the fact that at 40 km/h Mechanism 4 occurs frequently with the lowest values of the ratio BLEH/Ped. Height and Mechanism 5b is the most common for the lowest values of the ratio BLEH/Ped. Height. As a consequence of this the highest head-ground impact speed values are found at the upper and lower bounds of the interval, while the lower values are located in correspondence of the central part of the interval; hence, the weak parabolic relationship between head-ground impact speed and BLEH/Ped. Height.

Considering only impacts with the adult male pedestrian, Fig. 14 B shows head-ground impact speed increases with NBLEH at 20 and 30 km/h, however R^2 values are low (0.20 at 20 km/h and 0.11 at 30 km/h). No relationship between head impact speed and NBLEH is evident for males at 40 km/h. For the adult female pedestrian no relationship between head-ground impact speed and NBLEH could be identified at any vehicle impact speed. For the child pedestrian impact cases the relationships are stronger, with an increasing linear relationship at 20 km/h and 30 km/h ($R^2 = 0.43$ and $R^2 = 0.41$ respectively) and a quadratic relationship at 40km/h ($R^2 = 0.53$).

4.3 - *Relationship between vehicle impact speed and ground impact mechanism*

At 20 km/h, Fig. 14 (B and C) shows that Mechanism 2 (average head impact speed 3.2 m/s) is the most frequent outcome with adult pedestrians for all vehicle types (89% of cases for the male pedestrian and 85% of cases for the female pedestrian). At this low speed a head-first impact with the ground (Mechanism 1) is unlikely because rotation of the pedestrian after primary impact

353 is insufficient to raise the pelvis above the head prior to ground impact. Thus serious head injury from ground contact is less
354 likely in these cases.

355 At 30 km/h there are fewer instances of Mechanism 2 and more of Mechanism 1 (average head impact speed 4.6 m/s) for adult
356 pedestrians (see Fig. 14 B and C), especially for the lower fronted vehicles (NBLEH < 0.6), since the increased speed causes
357 more whole-body rotation. Thus adult head injuries from ground contact are likely to increase when vehicle speeds increase from
358 20 to 30 km/h. For child pedestrians, there are many Mechanism 5b cases at 30 km/h for the higher fronted vehicles (NBLEH >
359 0.6), and these are associated with very high head impact speeds (6.2 m/s on average). Thus, these are likely to be serious head
360 injury cases.

361 At 40 km/h there are many cases of Mechanisms 2 and 3 for adult pedestrians for the lower fronted vehicles (NBLEH < 0.5),
362 see Fig 14 B and C. In contrast, for higher fronted vehicles (NBLEH > 0.6) there are many cases of Mechanism 2. Since
363 Mechanisms 2 and 3 have relatively low head ground impact speeds, this is consistent with empirical evidence that head ground
364 injuries do not increase proportionately with vehicle impact speed (Ashton and Mackay 1983).

366 4.4 - *Relationship between vehicle type and ground impact mechanism*

367 There is a significant difference in the distribution of impact mechanisms between the low-fronted vehicles represented by the
368 three car models and the high-fronted vehicles represented by the two SUVs and the van. With the three car models the adult
369 pedestrian is impacted below the pelvis and the kinematic outcome of the impact is always a wrap-type trajectory. With the small
370 SUV, the first impact with vehicle front occurs around the pelvis and less whole body rotation is imparted to the pedestrian. With
371 the big SUV and the van, the vehicle front impacted the child pedestrian above the centre of gravity, resulting in forward
372 projection trajectories.

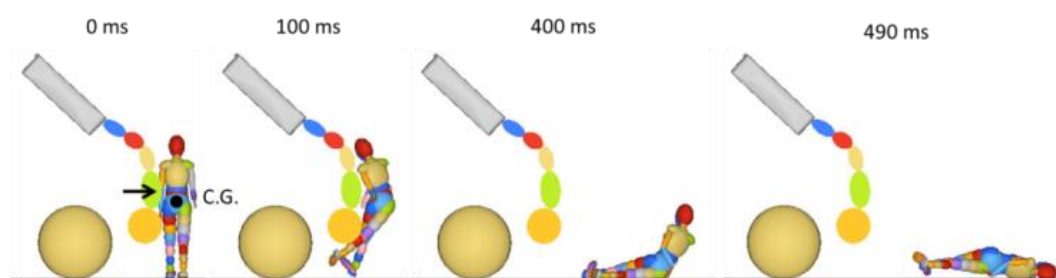
373 Fig. 6 shows that the instances of Mechanism 1 (head-first ground impact) for adult pedestrians (50th percentile male and 5th
374 percentile female) generally increase with increasing vehicle front height, except for the van model: for the sports car, Mechanism
375 1 occurred in 7 cases (10%) compared to 33 cases (45%) for the big SUV. For the van model, the most common impact
376 mechanism was Mechanism 2 (61%).

377 The distribution of ground impact mechanism among vehicle types for adults depends on vehicle impact speed. At 20 km/h,
378 Mechanism 2 is the most common for all vehicle types (91% with the sports car, 96% with the compact car and the big car, 87%
379 with the small SUV, 91% with the big SUV and 58% with the van). In contrast, at 30 km/h (Fig. 8), Mechanism 1 is much more
380 frequent than Mechanism 2, occurring in 17 cases (71%) with the compact car, and in 20 cases (83%) with the small SUV,
381 although in only 5 cases (21%) with the van (where Mechanism 2 dominates at this speed (75%). At 40 km/h (Fig. 9) impact
382 mechanisms characterized by high rotation of the pedestrian prior to ground contact (Mechanism 3 and 4) are most common with
383 the three car models: for example Mechanism 4 occurred in 18 cases (75%) of impacts with the sports car, 16 cases (66%) with

384 the compact car and 12 cases (50%) with the big car. Mechanism 3 never occurred with the sports car while it occurred in 7 cases
385 (29%) with the compact car, 6 cases (25%) with the big car, and 11 cases (45%) with the small SUV. Mechanism 1 remains
386 frequent with the two SUVs: 9 cases (37%) with the small SUV and 18 cases (75%) with the big SUV. For the van, Mechanism 1
387 & 2 dominate at this speed.
388

389 For the child pedestrian cases, Mechanism 2 accounts for around 40% of cases from the sports car up to the small SUV, while
390 Mechanism 5b dominates for the large SUV (89%) and van (100%). Again there is a speed dependency to these findings. At 20
391 km/h, only Mechanism 2 occurred with the three car models, while with the small SUV 8 cases of Mechanism 2 (67%) were
392 observed. In impacts with the big SUV and the van the outcome at this speed was always Mechanism 5b. At 30 km/h (see Fig. 12)
393 Mechanism 1 dominated for the compact car, while Mechanism 2 was very frequent for the big car and small SUV. Mechanism
394 5b dominated for the big SUV and van. At 40 km/h (see Fig. 13), Mechanism 1 is only common for the big car (50%).
395 Mechanism 2 only occurs for the small SUV, while Mechanism 3 is common for the compact car (50%). Mechanism 4 dominates
396 (83%) for the sports car, but the incidence is reduced to 2 cases (16.5 %) for the big car and there are no instances of Mechanism
397 4 for the small SUV, big SUV and van. Mechanism 5b dominates for the big SUV and van.

398 In the cases of Mechanism 5b the vehicle pushes the pedestrian forward and rotates the upper body towards the ground
399 (clockwise in Fig. 17). As a result, the pedestrian has a high head-ground impact speed (average 6.2 m/s) even at relatively low
400 vehicle impact velocities of 20 and 30 km/h. This weak dependence of head ground impact speed on vehicle impact speed in these
401 cases may be explained by the following: the vertical component of head velocity results from the combined effects of gravity and
402 whole-body rotation. Whole-body rotation occurs due to eccentric vehicle impact force and this is more pronounced at higher
403 speeds. However, at lower speeds the time to ground contact after the separation from the vehicle is longer and vertical head
404 velocity is accumulated through the action of gravity, which acts over a longer time than in the higher speed cases. The net effect
405 is that the head ground contact speed is similar across a broad range of speeds from 20-40 km/h for these cases. Thus vehicles
406 with a high bonnet leading edge relative to the pedestrian height might represent a serious threat to pedestrians in terms of
407 ground-related injuries even at low impact velocities.
408



409
410 **Fig. 17: Impact between the van and the child pedestrian at 20 km/h. The ground impact mechanism is Mechanism 5b.**
411

412 4.5 - Relationship between vehicle front height and head-ground impact speed in head-first impacts with ground

413 The linear regression analysis performed on the 77 cases of Mechanism 1 at 30 km/h (Fig. 15 A), shows a high correlation
414 between the head-ground impact speed and the NBLEH ($R^2=0.56$) and almost a doubling of head impact speed between the
415 lowest and highest values of NBLEH. This suggests that within Mechanism 1 cases (which account for two thirds of adult cases at
416 30 km/h) the higher bonnet leading edge heights of SUVs and vans induces significantly higher head ground impact speeds.

417 This can also be seen in Table 7, which shows a consistent increase in average head ground impact speed from 3.8 m/s for the
418 sports car up to 5.6 m/s for the van. In addition the strong ($R^2 = 0.61$) negative correlation of the time between first contact with
419 the vehicle and the head-ground impact with the NBLEH (Fig. 15 B), shows that high-fronted vehicles are associated with earlier
420 impacts with the ground in these cases, and a consistent trend exists for the average values of time to head-ground impact for each
421 vehicle type (see Table 7). Not surprisingly, therefore, a linear regression between head ground impact speed and time to head
422 contact (Fig. 15 C) also yields a high correlation ($R^2 = 0.41$), with shorter times to head ground generally yielding higher head
423 impact speeds.

424 Mechanism 1 also occurred at 40 km/h in 37 cases (2 with the big car, 9 with the small SUV, 18 with the big SUV and 8 with
425 the van); if these cases are included in the linear regression analysis the same relationships described above hold, with $R^2 = 0.55$
426 between NBLEH and head-ground impact speed, $R^2 = 0.61$ between NBLEH and time to head-ground impact and $R^2 = 0.38$
427 between head-ground impact speed and time to head-ground impact.

428
429 **Table 7. Average values of head-ground impact speed for the 77 cases of Mechanism 1 resulting from impacts at 30**
430 **km/h with adult pedestrians.**

Vehicle	Avg. head-ground speed (m/s)	Avg. time to head-ground impact (ms)	Number of cases
Sports car	3.8	872	7
Compact car	4.3	842	17
Big car	4.4	831	13
Small SUV	5.4	768	20
Big SUV	5.3	702	15
Van	5.6	712	5

431
432 Fig. 8 and Fig. 9 show that a head-first impact with the ground (Mechanism 1) is a likely outcome for adult pedestrians with all
433 vehicle types at 30 km/h and with high-fronted vehicles at 40 km/h, but Fig. 15 and Table 7 indicate that the head-ground impact
434 speed is higher in cases with high-fronted vehicles. The reason for this may be related to the fact that for low-fronted vehicles the
435 head-ground impact occurs later than for high-fronted vehicles and there is therefore a longer pedestrian interaction with the
436 vehicle front before separation and ground contact occur. In particular when the bonnet leading edge is lower than the pelvis, the
437 pedestrian wrap trajectory leads to further interaction with the vehicle which reduces the whole-body angular velocity and hence
438 the head-ground impact speed.

4.6 - *Effects of pedestrian initial stance and walking speed*

The pedestrian initial stance and walking speed introduced a substantial variability in the simulation results and in some cases for similar impact scenarios changed the outcome of the impact from potentially life-threatening for the pedestrian to non-severe.

As visible in figure 14, the main effect of changing pedestrian initial stance and walking speed with all the other parameters being the same was to introduce a variation in pedestrian post-impact kinematics such to lead to a different Mechanism of impact with ground (e.g. male pedestrian at 30 km/h with BLE/Ped. Height = 0.398) or to the same ground Impact Mechanism but with significantly different head-ground impact speeds (e.g. female pedestrian at 40 km/h with BLE/Ped. Height = 0.473).

These results indicate that the variability introduced by pedestrian initial stance and walking speed cannot be neglected and therefore the trends identified in this study should not be used as a predictive tool for head injury assessment for a specific collision scenario

4.7 - *. Limitations of the study*

Validated contact characteristics based on the deformation properties of bonnet, bumper and windscreen were used to model pedestrian-vehicle contact interaction (Lyons and Simms 2012). These contact functions were developed to generate reasonable contact forces in the pedestrian/vehicle interaction. However, they did not account for differences in stiffnesses between vehicle types, as well as for the presence of regions of localised stiffness on the bonnet. In addition, vehicle braking effects were not included in the modelling, and these have some effect on pedestrian kinematics.

Three different pedestrian sizes were used to account for the differences in impact kinematics due to different bonnet height/pedestrian height ratios. The mid-size 50% male model has been extensively validated, while the small female and the child, obtained by scaling the mid-size male model, were not validated.

Most importantly, the MADYMO pedestrian models are not validated in terms of kinematic response for the interaction with the road, since such validation data is unfortunately not in the public domain.

5 - Conclusions

On the basis of the multibody modelling performed in this work using the 50th % adult male, the 5th % adult female and the 6 year old child MADYMO pedestrian models in simulated impacts with a range of vehicle types and a range of initial pedestrian gait stances and transverse speeds at vehicle impact speeds of 20-40km/h the following conclusions can be drawn:

1. Despite the high variability observed in pedestrian-ground contact, it is possible to identify six recurring configurations of pedestrian impact with the ground in 97% of the impact simulations performed. These configurations have statistically distinct and considerably different average head-ground impact speeds.
2. At 20 km/h vehicle impact speed the most common event for adult pedestrians is a wrap trajectory after which the pedestrian strikes the ground with the lower body first, followed by the torso and the head. A head-first impact is generally avoided.
3. At 30 km/h a head-first impact with the ground for adults is likely for all vehicle types except the sports car and the van. When this mechanism occurs, the head-ground impact speed increases linearly and substantially with normalized bonnet leading edge height. Thus vehicles with a high bonnet leading edge relative to the pedestrian height are likely to cause higher head ground contact speeds at 30km/h.
4. At 30km/h, when adult head-first impacts with the ground cannot be avoided, low-fronted vehicles (cars) provide a better containment of the pedestrian on the bonnet, ultimately reducing the head-ground impact speed.
5. SUVs and vans appear to be more aggressive for head-ground contact to adult pedestrians than cars when the impact speed is at or below 30 km/h. At 40 km/h low-fronted vehicles cause whole body rotations in excess of 270° and high average head-ground impact speeds for adult pedestrians. These results indicate that at 40km/h a low front might not give any benefit in terms of reducing the severity of head-ground impact.
6. For child pedestrians, a forward projection trajectory with high ground impact speed was observed for high fronted vehicles.

References

- Anderson, R., Streeter, L., Ponte, G., Mclean, A., 2007. Pedestrian reconstruction using multibody madymo simulation and the polar ii dummy: A comparison of head kinematics. In: Proceedings of the 20th International Technical Conference on the Enhanced Safety of Vehicles (ESV), Lyon, France, pp. 1-15.
- Ashton, S., Mackay, G., 1983. Benefits from changes in vehicle exterior design: Field accident and experimental work in europe. Society of Automotive Engineers, SAE Paper No. 830626.

492 Ballesteros, M.F., Dischinger, P.C., Langenberg, P., 2004. Pedestrian injuries and vehicle type in maryland, 1995–
493 1999. *Accident Analysis & Prevention* 36 (1), 73-81.

494 Chidester, A.B., Isenberg, R.A., 2001. Final report-the pedestrian crash data study. In: *Proceedings of the*
495 *Proceedings of the 17th International Enhanced Safety Vehicle Conference*, Amsterdam, The Netherlands.

496 Elliott, J.R., 2011. Monte carlo modelling to estimate pedestrian pre-impact velocity from post-accident vehicle
497 damage. MSc. Thesis. Trinity College Dublin.

498 Elliott, J.R., Simms, C.K., Wood, D.P., 2012. Pedestrian head translation, rotation and impact velocity: The influence
499 of vehicle speed, pedestrian speed and pedestrian gait. *Accident Analysis and Prevention* 45, 342-53.

500 Euroncap, 2013. European new car assessment programme (euroncap). Pedestrian testing protocol.

501 Gupta, V., Yang, K.H., 2013. Effect of vehicle front end profiles leading to pedestrian secondary head impact to
502 ground. *Stapp Car Crash Journal* 57, 139-155.

503 Hamacher, M., Eckstein, L., Paas, R., 2012. Vehicle related influence of post-car impact pedestrian kinematics on
504 secondary impact. IRCOBI Conference. Dublin, pp. 717-729.

505 Happee, R., Haaster, R., L, M., R, H., 1998. Optimisation of vehicle passive safety for occupants with varying
506 anthropometry. *ESV Conference*.

507 Jarrett, K., Saul, R., 1998. Analysis of the pcds field collision data. In: *Proceedings of the 16th International Technical*
508 *Conference on the Enhanced Safety of Vehicles (ESV)*, Windsor, Ontario, Canada.

509 Kendall, R., Meissner, M., Crandall, J., 2006. The causes of head injury in vehicle-pedestrian impacts: Comparing the
510 relative danger of vehicle and road surface. *SAE Technical Paper* 2006-01-0462.

511 Kerrigan, J., Arregui-Dalmases, C., Crandall, J., 2012. Assessment of pedestrian head impact dynamics in small
512 sedan and large suv collisions. *International Journal of Crashworthiness* 17 (3), 243-258.

513 Kerrigan, J.K., Murphy, D.B., Drinkwater, D.C., Kam, C.Y., Bose, D., J, C., 2005a. Kinematic corridors for pmhs tested
514 in full-scale pedestrian impact tests. In: *Proceedings of the Conference on the Enhanced Safety of Vehicles*
515 *(ESV)*, Washington DC, United States.

516 Kerrigan, J.R., Kam, C.Y., Drinkwater, D.C., Murphy, D.B., Bose, D., Ivarsson, B.J., Crandall, J.R., 2005b. Kinematic
517 comparison of the polar-ii and pmhs in pedestrian impact tests with a sport-utility vehicle. IRCOBI Conference
518 on the Biomechanics of Impact. Prague, Czech Republic.

519 Linder, A., Douglas, C., Clark, A., Fildes, B., Yang, J., Otte, D., 2005. Mathematical simulations of real-world
520 pedestrian-vehicle collisions. In: *Proceedings of the Proceedings of the 19th International Technical*
521 *Conference on the Enhanced Safety of Vehicles (ESV)*, Washington, D.C, Paper No. 05-285.

522 Liu, X., Yang, J., Lovsund, P., 2002. A study of influences of vehicle speed and front stucture on pedestrian impact
523 responses using mathematical models. *Traffic Injury Prevention* (3), 31-42.

524 Longhitano, D., Henaray, B., Bhalla, K., Ivarsson, J., Crandall, J., 2005. Influence of vehicle body type on pedestrian
525 injury distribution. *Society of Automotive Engineers*, Preliminary Paper number 05B-409.

526 Lopez, A.D., Mathers, C.D., Ezzati, M., Jamison, D.T., Murray, C.J.L., 2006. Global and regional burden of disease
527 and risk factors, 2001: Systematic analysis of population health data. *The Lancet* 367 (9524), 1747-1757.

528 Lyons, M., Simms, C.K., 2012. Predicting the influence of windscreen design on pedestrian head injuries. IRCOBI
529 Conference. pp. 1-14.

530 Madymo, 2011. Madymo theory manual v7.4, Delft, The Nedherlands.

531 Mizuno, K., Kajzer, J., 1999. Compatibility problems in frontal, side, single car collisions and car-to-pedestrian
532 accidents in japan. *Accident Analysis and Prevention* 31 (4), 381-391.

533 Moore, D.S., Mccabe, G.P., 2003. *Introduction to the practice of statistics (4e)* W H Freeman & Co.

534 Otte, D., Pohlemann, T., 2001. Analysis and load assessment of secondary impact to adult pedestrians after car
535 collisions on roads. In: Proceedings of the IRCOBI Conference, Isle of Man.

536 Roudsari, B.S., Mock, N.C., Kaufman, R., 2005. An evaluation of the association between vehicle type and the source
537 and severity of pedestrian injuries. *Traffic Injury Prevention*.

538 Shen, J., Jin, X.L., Zhang, X.Y., 2008. Simulated evaluation of pedestrian safety for flat-front vehicles. *International*
539 *Journal of Crashworthiness* 13 (3), 247-254.

540 Simms, C.K., Ormond, T., Wood, D.P., 2011. The influence of vehicle shape on pedestrian ground contact
541 mechanism. In: Proceedings of the IRCOBI Conference, Dublin.

542 Simms, C.K., Wood, D.P., 2006a. Effects of pre-impact pedestrian position and motion on kinematics and injuries
543 from vehicle and ground contact. *International Journal of Crashworthiness* 11 (4), 345-355.

544 Simms, C.K., Wood, D.P., 2006b. Effects of pre-impact pedestrian position and motion on kinematics and injuries
545 from vehicle and ground contact. *International Journal of Crashworthiness* 11 (4), 345-356.

546 Simms, C.K., Wood, D.P., 2006c. Pedestrian and cyclist impact mechanics, Dublin.

547 Simms, C.K., Wood, D.P., 2006d. Pedestrian risk from cars and sport utility vehicles - a comparative analytical study.
548 Proceedings of the Institution of Mechanical Engineers, Part D: Journal of Automobile Engineering 220 (8),
549 1085-1100.

550 Subit, D., R, K.J., Crandall, J.R., Fukuyama, K., Yamazaki, K., Kamiji, K., Yasuki, T., 2008. Pedestrian-vehicle
551 interaction: Kinematics and injury analysis of four full-scale tests. IRCOBI Conference on the Biomechanics of
552 Impact. Bern, Switzerland.

553 Untaroiu, C.D., Crandall, J.R., Takahashi, Y., Okamoto, M., Ito, O., Fredriksson, R., 2010. Analysis of running child
554 pedestrians impacted by a vehicle using rigid-body models and optimization techniques. *Safety Science* 48
555 (2), 259-267.

556 Untaroiu, C.D., Meissner, M.U., Crandall, J.R., Takahashi, Y., Okamoto, M., Ito, O., 2009. Crash reconstruction of
557 pedestrian accidents using optimization techniques. *International Journal of Impact Engineering* 36 (2), 210-
558 219.

559 Van Rooij, L., Bhalla, K., Meissner, M., Ivarsson, M., Crandall, J., 2003. Pedestrian crash reconstruction using multi
560 body modelling with geometrically detailed, validated vehicle models and advanced pedestrian injury criteria.
561 In: Proceedings of the Proceedings of the 18th International Technical Conference on the Enhanced Safety of
562 Vehicles, Nagoya, Japan.

563 Wood, D.P., Simms, C.K., 2000. Coefficient of friction in pedestrian throw. *Impact, Journal of ITAI* 9 (1), 12-14.

564 World Bank. *World bank group: Road safety*, (2002). Retrieved: September 9, 2013, from
565 <http://www.worldbank.org/transport/roads/safety.htm>

566 Yao, J., Yang, J., Otte, D., 2008. Investigation of head injuries by reconstructions of real-world vehicle-versus-adult-
567 pedestrian accidents. *Safety Science* 46 (7), 1103-1114.

568